Enhanced photocatalytic activity of $Au@SiO_2/TiO_2$ by promoted LSPR

Jiun-Jen Chen[a] Jeffrey C.S. Wu*[a], Pin Chieh Wu[b], and Din Ping Tsai[b]

[a]Department of Chemical Engineering, National Taiwan University
[b]Department of Physics, National Dong Hwa University
*Email: cswu@ntu.edu.tw

Abstract

The photocatalytic activity was enhanced on the TiO_2 film as a result of the Localized Surface Plasmon Resonance (LSPR) being promoted by the Au particles covered with SiO_2 shell. The Au core with 3 nm SiO_2 shell was loaded onto the TiO_2 film. The photocatalytic activities of Au/TiO_2, $Au@SiO_2/TiO_2$, and TiO_2 films were evaluated by the degree of photodegradation of methylene blue (MB) under similar conditions with UV-visible light irradiation for 5 h. The degree of MB photodegradation was in the following order: $Au@SiO_2/TiO_2>Au/TiO_2>TiO_2$. $Au@SiO_2/TiO_2$ reached 95% MB photodegradation after 5 h with light irradiation. Although SiO_2 shell insulated the electron trap effect, the MB photodegradation on $Au@SiO_2/TiO_2$ was superior to Au/TiO_2 because its LSPR is much higher than that of the Au/TiO_2. To further confirm the validity of the experiment result, the LSPR of Au with SiO_2 shell was illustrated by finite element method electromagnetic simulation. $Au@SiO_2/TiO_2$ showed nearly 9 times of increase in EM field comparing to Au/TiO_2.

Keywords: Photocatalysis, Gold nanoparticle, Local surface plasmon resonance, TiO_2, SiO_2.

1 Introduction

Nowadays, semiconductor photocatalysis attracts a considerable amount of studies due to its applications in modern catalytic research. In particular, environmental applications of TiO_2 has attracted much attention because it is one of the most affordable, stable, and active photocatalysts. Many researchers tried to improve the photocatalytic performance of TiO_2, one of the methods being modification with noble metals**[1-5].** In the use of photocatalysts to carry out photocatalytic reactions, nanoparticles loaded on TiO_2 often behave as electron traps **[4, 6].**

The noble metal nanoparticles are different from their bulk counterparts because of their small size, featuring unique electrical, mechanical, magnetic and optical properties. In particular, the optical properties of gold nanoparticles are dominated by their LSPR, defined as the collective motions of the conduction electrons induced by light irradiation **[7, 8].** This is associated with a considerable enhancement of the electric near-field. The resonance wavelength strongly depends on the size and shape of the nanoparticles, the interparticle distance, and the dielectric property of the surrounding medium **[9, 10].** The LSPR effect of noble metal nanoparticles can also enhance the activity of photocatalytic reaction **[6, 11].**

Recently, the coating of silica shell on nanoparticles has been widely discussed because it has the following advantages: it acts as a bridge to provide the cores with different reaction sites, it tunes the optical properties of the cores, and it increases the stability of nanoparticle dispersion **[12-14].** These recent studies gave us insight into the composite structure of silica-coated nanoparticles, the easily modified silica surface, and the unique properties of nanoparticles. Compared to the large efforts made towards the thickness optimization of silica shells and the study of their surface morphology **[15, 16],** less research has explored the effect of SiO_2 on LSPR effect for nanoparticle core.

To further understand the role of Au nanoparticles in photocatalytic reaction and the effect of SiO_2 coating on such nanoparticles, several plasmonic photocatalysts were fabricated. Plasmonic photocatalysts, $Au@SiO_2/TiO_2$, Au/TiO_2, and TiO_2 film were prepared and MB photodegradation was conducted to determine the

photocatalytic activity. Furthermore, simulation was carried out to give insight into the possible changes of the LSPR effect on Au nanoparticles with SiO_2 shell.

2 Experimental

A gold dispersion was prepared according to the sodium citrate reduced method, this method produced a stable, deep-red suspension of gold particles. An aqueous solution of 3-aminopropyltrimethoxysilaneaps (APS, 5 mL, 1 mM) was added to 500 mL of the gold solution under vigorous magnetic stirring. The mixture of APS and gold dispersion was left to stand for 15 min to allow complete complexation of the amine groups with the gold surface. By progressive addition of cation exchange resin, a solution of active silica was produced by lowering the pH of a 0.54 wt% sodium silicate solution to 10.5. After which, 10 mL of active silica was released into 500 mL of the surface modified gold solution under vigorous magnetic stirring. The silica shell with thickness of near 3 nm was obtained by allowing the solution to stand for over 2 days prior to the removal of free silicates via centrifugation, so that further growth of silica could be prevented.

The TiO_2 sol was obtained by the thermal hydrolysis method. Tetrabutoxide titanate (TBOT) and polyethylene glycol (PEG) were added to 0.1 M nitric acid (HNO_3) solution. The volume of HNO_3 was six times of that of TBOT, and the weight of PEG was half of that of TiO_2. The mixed solution was heated to 80°C and kept at the same temperature for 8 h. A thin TiO_2 film was prepared by dip coating on the quartz plate. The TiO_2 film coated on quartz plate was then calcined. A pipet was used to take either 4 mL of Au dispersion or 4 mL of Au@SiO_2 dispersion solution, and spread the solution on the TiO_2 quartz plate. To increase the adhesion of nanoparticles on the plate, the resulting sample was heated from room temperature to 80°C.

TEM of the nanoparticles was carried out on a Hitachi model H-7100 instrument. Dynamic light scattering measurements were performed on a Zetasizer Nano ZS analyzer (Malvern). The light absorption of nanoparticles was characterized by diffusive reflective UV-vis spectroscopy (Varian, Cary 100). FE-SEM and energy dispersive spectroscopy were performed on the Hitachi model S-800.

The MB aqueous solution was photo degraded in a glass reactor at 25°C. The photocatalysts-deposited quartz plate was immersed in the solution and irradiated simultaneously by UV (365 nm) and the Xe lamp with filter (400 nm < λ < 700 nm). The intensity of the visible light was 150 klux. UV-vis spectroscopy (Cary 100, Varian) was used to measure the concentration of the MB aqueous solution based on the intensity of the absorption peak at 664.3 nm.

All of the simulated spectra and electromagnetic field distribution were obtained by solving three-dimensional Maxwell equations with the commercial COMSOL Multiphysics software, which is based on finite element method.

3 Result and Discussion

3.1. Photocatalyst characterization

Before coating, the diameter of the Au core was 18 nm based on the TEM results shown in Fig. 1(a). Fig. 1(b) shows a TEM micrograph of the nanoparticles with Au core average diameter of 50 nm and silica shell thickness of near 3 nm. The reason why the Au core increased from 18 nm to 50 nm is because of the constant stirring of Au particles, causing the growth of Au particle size during the procedure. Complete silica shell was formed and the thickness was measured to be 3 nm for most spherical particles of Au cores resulting in a total diameter of 56 nm for the nanoparticles. The size distribution of the bare Au and Au@SiO_2 were measured via DLS. As can be seen in Fig. 2, the average size of bare Au is measured to be 35 nm and that of Au@SiO_2 is measured to be 65 nm. The particle size determined from DLS is larger than that determined from the TEM measurement. This is due to the fact that DLS takes the hydrodynamic diameter into account, i.e. the diameter of a hypothetical hard sphere diffusing at the same rate as the particle in the fluid. Another reason may be the slight aggregation of the primary particles. It was difficult to obtain large amount of Au@SiO_2 nanoparticles with uniform size distribution. Compared to the TEM results, the DLS results are wider ranged and more precise. Thus, the size measured by DLS was used in further simulations.

Au is well known for having attractive optical properties. The optical extinction of Au is due to a collective oscillation of the free electrons known as the plasmon resonance. Fig. 3 shows the bare Au nanoparticles giving a

characteristic surface plasmon at 523.8 nm. As silica shell encapsulates the Au surface, there is an increase in the intensity of the plasmon absorption and a red shift in the position of the maximum band. The peak of Au was shifted to longer wavelength. This is due to an increase in the local refractive index around the nanoparticles by the silica shell, resulting in the maximum adsorption peak of Au@SiO_2 at 526 nm as shown in Fig. 3.

As above depicted, the absorbance and the position of the maximum absorption of Au@SiO_2 nanoparticles can be adjusted by adding a silica shell, or by controlling the thickness of the silica shell. These phenomena have been investigated in detail by Liz-Marz´an and co-workers **[17].** In a word, such phenomena are of extreme importance if one wants to use the optical properties of Au.

The bright spots that can be seen in Fig. 4 are the slightly aggregated Au@SiO_2. The aggregation was caused by the heat from the drying procedure. The Au@SiO_2 dispersion is loaded onto the TiO_2 film.

3.2 MB photodegradation

Fig. 5 shows the result of the photodegradation of MB solution under simultaneous UV and visible-light irradiation. Factors affecting MB concentration to decrease in the solution can be categorized into three kinds **[6].** First is the physical adsorption of MB on the photocatalysts, second is the photodegradation of MB by light irradiation alone, and third is the photocatalytic degradation of MB in the solution **[4,18-20]**. The control experiment with only UV+visible light irradiation achieved MB degradation efficiency of near 15% in 5 h, whereas the MB degradation efficiency was increased in the presence of different photocatalysts. When TiO_2 film was immersed into the MB solution, the photocatalytic degradation efficiency reached near 44% in 5 h of UV+visible light exposure because TiO_2 is activated by UV light. The MB degradation efficiency of Au/TiO_2 increased to near 80% in 5 h of UV+visible light exposure because the Au nanometals can serve as electron traps **[4].** Under UV light irradiation, the photogenerated electrons are transferred from the TiO_2 conduction band to the Au, and the holes are accumulated in the TiO_2 valence band. Hence, photogenerated electrons and holes are efficiently separated. This prolongs the lifetime of electrons and holes thus increase the photocatalytic reaction activity. Besides that, MB photodegradation was also enhanced by the LSPR effect from the Au as it was irradiated by visible light **[6,11].** On the other hand, the introduction of Au@SiO_2/TiO_2 achieved MB degradation efficiency of 95% under UV+visible light irradiation in 5 h. The coating of SiO_2 insulated the Au particles, thus blocked out the photogenerated electrons from TiO_2. In this case, Au can no longer play the role of electron trap. However, the MB photodegradation efficiency of the Au@SiO_2/TiO_2 is the highest among all. Therefore, we can deduce that the SiO_2 coating further promotes the LSPR of Au compared to that of bare Au. Au nanoparticle is well known to produce an enhanced spatially confined electrical field close to the particle surface. This is mainly due to the collective oscillation of the electrons on the conduction band. According to Kumar and his co-workers **[16],** the coupling of the LSPR of nanometals (Ag) with the band gap of TiO_2 conducts energy transfer, in which the plasmon relaxation occurs via excitation of electron-hole pairs in the TiO_2. Such EM field relaxation channel will appear if the plasmon energy is larger than the band gap of TiO_2. However, the EM field will remain “inert” to the field if the surrounding medium is an insulator (e.g., SiO_2) with a larger band gap than the plasmon excitation energy. For the optimal application of this system, a maximum overlap must be made with the LSPR band and the bandgap of TiO_2. Adding a SiO_2 shell promotes the overlap and is beneficial to the system. However, increasing SiO_2 thickness may cause the reduction of penetration depth. Therefore, authors concluded that a 2-5 nm SiO_2 interlayer between the Ag nanoparticles and the TiO_2 film was optimal for reaching maximum EM energy coupling. Furthermore, they mentioned that SiO_2-promoted LSPR not only creates more e^-/h^+ pairs but also prevents their recombination.

In some studies, the addition of SiO_2 in TiO_2 was reported to increase the surface area of TiO_2 particles, enhance the thermal stability for the phase of TiO_2 particles, and raise the surface acidity, resulting in enhanced MB photodegradation. These effects are due to the inclusion of SiO_2 in the process of TiO_2 fabrication. However, in our study, we did not add SiO_2 until the TiO_2 film was completely formed. The presence of SiO_2 on TiO_2 film would not change the chemical properties of TiO_2. Moreover, the differences in MB photodegradation efficiency between TiO_2, Au/TiO_2, and Au@SiO_2/TiO_2

were not due to the different adsorption capacity of these photocatalysts. As can be seen in Fig. 5, three photocatalysts have a similar MB removal of within 3~4% when they are placed in the solution without light irradiation. The 3-nm SiO_2 shell has insignificant effect on increasing the adsorption of MB. Therefore, in the $Au@SiO_2/TiO_2$, the 3-nm SiO_2 shell plays an important role to promote the LSPR, thus significantly increasing the photocatalytic activity.

3.3 LSPR simulation

To gain a deeper understanding on the effect of the energy transfer from nanoparticles to TiO_2, we simulated two nanoparticles on a TiO_2 thin film and investigated the spatial distribution of electric field intensity. Figure 6 shows the FEM simulation results of electric field intensity in arbitrary unit at x-z plane for Au nanoparticle dimer and $Au@SiO_2$ core-shell nanoparticle dimer at wavelength λ = 540 nm (left) and wavelength λ = 545 nm (right), respectively. The electromagnetic wave is incident from z to -z with x polarization in both cases shown in Fig. 6. The diameter of Au nanoparticles is 35 nm and that of $Au@SiO_2$ core-shell nanoparticles is 65 nm (including the thickness of SiO_2 shell), which are the average dimensions obtained from Fig. 2. As expected, due to the LSPR effect and near field coupling between nanoparticles, the spatial electric field enhancement can be observed in the both cases of Au and $Au@SiO_2$ nanoparticles. The electric field intensity on the outer surface of $Au@SiO_2$ core-shell nanoparticle is 8.98 times higher than that of bare Au nanoparticle. In our previous work**[6],** we pointed out that the Au nanoparticles play two kinds of roles in enhancing photocatalytic reaction process: (i) an electron trap to decrease the probability in the recombination of electron-hole pairs, and (ii) enhance near EM field intensity by LSPR to increase the photoreaction. Due to the SiO_2 insulator coated on the Au nanoparticles, the transfer of induced electron from TiO_2 thin film to metallic nanoparticles is hindered, which should make photocatalytic reaction rate lower. However, according to our measured data, we found that the photocatalytic reaction rate in the case of $Au@SiO_2/TiO_2$ is higher than that of Au/TiO_2. The plasmon induced oscillating electron in the case of $Au@SiO_2/TiO_2$ creates a higher and local electric field than the case of Au/TiO_2. Such promoted LSPR can assist in generating more electron-hole pairs inside the TiO_2 thin film to compensate for the loss of the electron trap effect due to SiO_2 insulation. This evidence proves that near field intensity enhancement of surface plasmon effectively increases the photocatalytic process.

(a) (b)

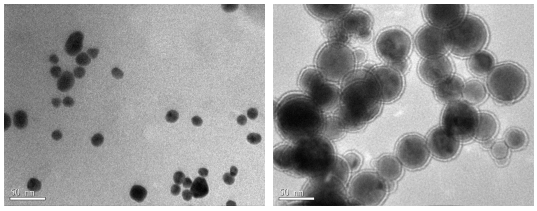

Figure 1: TEM photos of (a) bare Au with an average diameter of 18 nm, and (b) $Au@SiO_2$ with an average diameter of 56 nm.

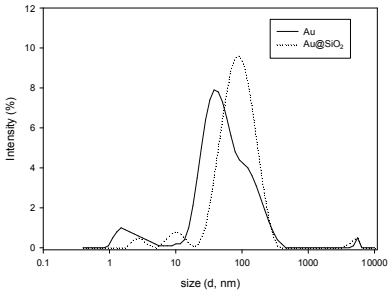

Figure 2: Particle size distribution of bare Au particles and $Au@SiO_2$ particles by dynamic light scattering

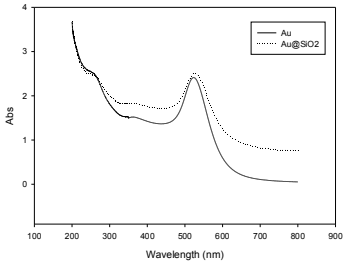

Figure 3: UV-vis spectrum of (a) bare Au with max peak at 523.8 nm, and (b) $Au@SiO_2$ with max peak at 526 nm

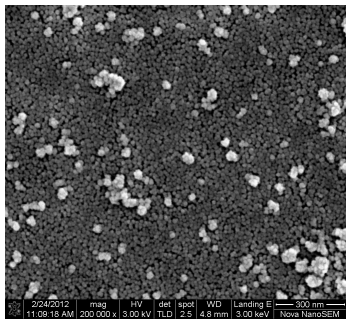

Figure 4: Top-view SEM image of $Au@SiO_2/TiO_2$

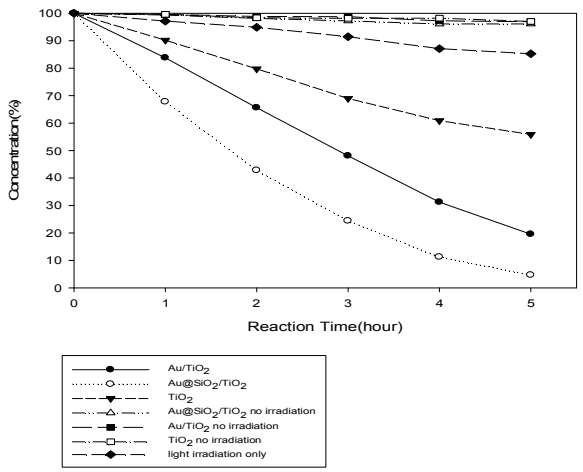

Figure 5: MB photodegradation under various conditions

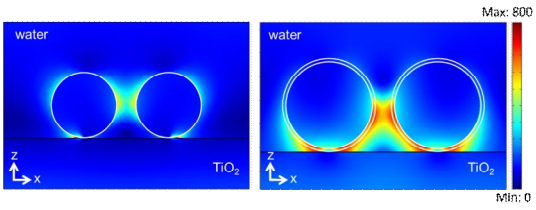

Figure 6: Simulation of electric field intensity under x-polarized illumination of gold nanoparticles only (left) and gold nanoparticles covered with 3 nm SiO_2 on TiO_2 in x-z plane (in arbitrary unit). The diameter of nanoparticles is 35 nm (without SiO_2) and 65 nm (with 3 nm SiO_2), respectively.

4 Conclusion

We have investigated the photocatalytic activity of different plasmonic photocatalysts, $Au@SiO_2/TiO_2$, Au/TiO_2, and TiO_2 by carrying out MB photodegradation. Three photocatalysts, TiO_2, Au/TiO_2, and $Au@SiO_2/TiO_2$ gave 44%, 80%, and 95% in MB photodegradation efficiency after 5 h of UV+vis light irradiation, respectively. $Au@SiO_2/TiO_2$ provided the best performance in the MB photodegradation. The reason why Au/TiO_2 performed better than TiO_2 film alone is because the Au particles acted as electron traps to inhibit electron-hole recombination, together with the LSPR effect of Au. On the other hand, the MB photodegradation efficiency of $Au@SiO_2/TiO_2$ was superior to that of Au/TiO_2 because the LSPR effect of the $Au@SiO_2/TiO_2$ is higher than that of the Au/TiO_2 even though the 3-nm SiO_2 shell insulated the Au and nullified its electron trap effect. In compliment with our findings, the simulated results showed approximately 9 times of increase in EM field comparing SiO_2-coated Au with bare Au. The SiO_2 shell played the role of enhancing the LSPR effect of Au under proper light irradiation.

Acknowledgments

The authors would like to acknowledge the National Science Council of Taiwan for financial support of this research under project number NSC 100-2120-M-002-008.

References

[1]Sreethawong, T.; Yoshikawa, S. "Comparative Investigation on Photocatalytic Hydrogen Evolution over Cu-, Pd-, and Au-loaded Mesoporous TiO_2 Photocatalysts", *Catal. Commun.* **2005**, *6*, 661-668.

[2]Kwak, B.-S.; Chae J.-H.; Kim, J.-E.; Kang, M.-S. "Enhanced Hydrogen Production from Methanol/Water Photo-Splitting in TiO2 Including Pd Component", *Bull. Korean Chem. Soc.* **2009**, *30*, 1047-1053.

[3]Kudo, A.; Miseki, Y. Heterogeneous "Photocatalyst Materials for Water Splitting", *Chem. Soc. Rev.* **2009**, *38*, 253-278.

[4]Yogi, C.; Kojima, K.; Takai, T.; Wada, N. "Photocatalytic Degradation of Methylene Blue by Au-deposited TiO_2 Film under UV Irradiation", *J. Mater. Sci.* **2009**, *44*, 821-827.

[5]Sasaki,Y.; Nemoto, H.; Saito, K.; Kudo. A. "Solar Water Splitting Using Powdered Photocatalysts Driven by Z-Schematic Interparticle Electron Transfer without an Electron Mediator", *J. Phys. Chem. C* **2009**, *113*, 17536-17542.

[6]Chen, J.-J.; Wu, J. C.-S.; Wu, P.-C; Tsai, D.-P. "Plasmonic Photocatalyst for H2 Evolution in Photocatalytic Water Splitting", *J. Phys. Chem. C* **2011**, *115*, 210-216.

[7]Wu, D.; Xu, X.; Liu, X. "Electric Field Enhancement in Bimetallic Gold and Silver Nanoshells", *Solid State Commun.* **2008**, *148*, 163-167.

[8]Merlen, A.; Gadenne, V.; Romann, J.; Chevallier, V.; Patrone, L.; Valmalette, J. C. "Surface Enhanced Raman Spectroscopy of Organic Molecules Deposited on Gold Sputtered Substrates", *Nanotechnology.* **2009**, *20*, 1-7.

[9]Link. S.; El-Sayed, M. A. "Spectral Properties and Relaxation Dynamics of Surface Plasmon Electronic Oscillations in Gold and Silver Nanodots and Nanorods",

J. Phys. Chem. B **1999**, *103*, 8410-8426.

[10]Noguez, C. "Surface Plasmons on Metal Nanoparticles The Influence of Shape and Physical Environment", *J. Phys. Chem. C* **2007**, *111*, 3806-3819.

[11]Awazu, K.; Fujimaki, M.; Rockstuhl, C.; Tominaga, J.; Murakami, H.; Ohki, Y.; Yoshida, N.; Watanabe, T. "A Plasmonic Photocatalyst Consisting of Silver Nanoparticles Embedded in Titanium Dioxide", *J. Am. Chem. Soc.* **2008**, *130*, 1676-1680.

[12]Ung, T.; Liz-Marza´n, L. M.; Mulvaney P. "Optical Properties of Thin Films of Au@SiO_2 Particles", *J. Phys. Chem. B* **2001**, *105*, 3441-3452.

[13]Lu, Y.; Yin, Y.-D.; Li, Z.-Y.; Xia, Y.-N. "Synthesis and Self-Assembly of AuSiO_2 Core Shell Colloids", *Nano Lett.* **2002**, *2*, 785-788.

[14]Mahalingam, V.; Onclin, S.; Pe´ter, M.; Ravoo, B. J. R.; Huskens, J.; Reinhoudt D. N. "Directed Self-Assembly of Functionalized Silica Nanoparticles on Molecular Printboards through Multivalent Supramolecular Interactions", *Langmuir.* **2004**, *20*, 11756-11762.

[15]Ye, J.; Van de Broek, B.; De Palma, R.; Libaers, W.; Clays, K.; Van Roy, W.; Borghs, G.; Maes, G. "Surface Morphology Changes on Silica-Coated Gold Colloids", *Colloid Surf. A: Physicochem. Eng. Asp.* **2008**, *322*, 225-233.

[16]Kumar, M. K.; Krishnamoorthy, S.; Tan, L.-K.; Chiam, S.-Y.; Tripathy, S.; Gao, H. "Field Effects in Plasmonic Photocatalyst by Precise SiO_2 Thickness Control Using Atomic Layer Deposition", *ACS Catalysis.* **2011**, *1*, 300-308.

[17]Liz-Marza´n, L. M.; Giersig, M.; Mulvaney, P. Synthesis of Nanosized Gold-Silica Core-Shell Particles. *Langmuir.* **1996**, *12*, 4329-4335.

[18]Surovtseva, N. I.; Eremenko A. M.; Smirnova, N. P.; Pokrovskii, V. A.; Fesenko, T. V.; Starukh, G. N. The Effect of Nanosizes Titania-Silica Film Composition on the Photostability of Adsorbed Methylene Blue Dye. *Theor. Exp. Chem.* **2007**, *43*, 235-240.

[19]Yu, Z.; Chuang, S. S.-C. The Effect of Pt on the Photocatalytic Degradation Pathway of Methylene Blue over TiO_2 under Ambient Conditions. *Appl. Catal. B: Environ.* **2008**, *83*, 277-285.

[20]Yogi, C.; Kojima, K.; Wada, N.; Tokumoto, H.; Takai, T.; Mizoguchi, T.; Tamiaki, H. Photocatalytic Degradation of Methylene Blue by TiO_2 Film and Au Particles-TiO_2 Composite Film. *Thin Solid Films.* **2008**, *516*, 5881-5884.